Contact optical nanolithography using nanoscale C-shaped apertures

Liang Wang, Eric X. Jin, Sreemanth M. Uppuluri, and Xianfan Xu

School of Mechanical Engineering, Purdue University, West Lafayette, Indiana 47907
xxu@ecn.purdue.edu

Abstract: C-shaped ridge apertures are used in contact nanolithography to achieve nanometer scale resolution. Lithography results demonstrated that holes as small as 60 nm can be produced in the photoresist by illuminating the apertures with a 355 nm laser beam. Experiments are also performed using comparable square and rectangular apertures. Results show enhanced transmission and light concentration of C apertures compared to the apertures with regular shapes. Finite difference time domain simulations are used to design the apertures and explain the experimental results.

OCIS codes: (220.3740) Lithography; (230.7390) Waveguides, planar

References

1. J. Aizenberg, J. A. Rogers, K. E. Paul, and G. M. Whitesides, "Imaging the irradiance distribution in the optical near field," Appl. Phys. Lett. **71**, 3773-3775 (1997).
2. M. M. Alkaisi, R. J. Blaikie, S. J. McNab, R. Cheung, and D. R. S. Cumming, "Sub-diffraction-limited patterning using evanescent near-field optical lithography," Appl. Phys. Lett. **75**, 3560-3562 (1999).
3. S. Y. Chou, P. R. Krauss, and P. J. Renstrom , "Imprint of sub-25 nm vias and trenches in polymers," Appl. Phys. Lett. **67**, 3114-3116 **(**1995).
4. S. Davy, and M. Spajer, "Near field optics: Snapshot of the field emitted by a nanosource using a photosensitive polymer," Appl. Phys. Lett. **69**, 3306-3308 (1996).
5. W. Srituravanich, N. Fang, C. Sun, Q. Luo, and X. Zhang, "Plasmonic Nanolithography**,"** Nano Lett. **4**, 1085-1088 (2004).
6. X. Luo, and T. Ishihara, "Surface plasmon resonant interference nanolithography technique," Appl. Phys. Lett. **84**, 4780-4782 (2004).
7. Z. Liu, Q. Wei, and X. Zhang, "Surface Plasmon Interference Nanolithography**,"** Nano Lett. **5**, 957-961 (2005).
8. E. H. Synge, "A Suggested Method for extending Microscopic Resolution into the Ultra-Microscopic Region," Philosophical Magazine. **6**, 356-362 (1928).
9. H. Bethe "Theory of diffraction by small holes," Phys. Rev. **66**, 163-182 (1944).
10. X. Shi, and L. Hesselink, "Mechanisms for Enhancing Power Throughput from Planar Nano-Apertures for Near-Field Optical Data Storage,**"** Jpn. J. Appl. Phys. **41**, 1632-1635 (2002).
11. E. X. Jin, and X. Xu, "Finite-Difference Time-Domain Studies on Optical Transmission through Planar Nano-Apertures in a Metal Film," Jpn. J. Appl. Phys. **43**, 407-417 (2004).
12. K. Sendur, W. Challener, and C. Peng, "Ridge Waveguide as a Near-field Aperture for High Density Data Storage," J. of Appl. Phys. **96**, 2743-2752 (2004).
13. E. X. Jin, and X. Xu, "Radiation transfer through nanoscale apertures," 2005 J. of Quantitative Spectroscopy and Radiative Transfer. **93**, 163-173 (2005).
14. E. X. Jin and X. Xu, "Obtaining super resolution light spot using surface plasmon assisted sharp ridge nanoaperture**,"** Appl. Phys. Lett.**86**, 111106 (2005).
15. P. J. Schuck, D. P. Fromm, A. Sundaramurthy, G. S. Kino, and W. E. Moerner, "Improving the Mismatch between Light and Nanoscale Objects with Gold Bowtie Nanoantennas**,"** Phys. Rev. Lett. **94**, 017402 (2005).
16. F. Chen, A. Itagi, J. Bain, D. D. Stancil, T. E. Schlesinger, L. Stebounova, G. C. Walker, and B. B. Akhremitchev, "Imaging of optical field confinement in ridge waveguides fabricated on very-small-aperture laser," Appl. Phys. Lett. **83**, 3245-3247 (2003).
17. J. A. Matteo, D. P. Fromm, Y. Yuen, P. J. Schuck, W. E. Moerner, and L. Hesselink, "Spectral analysis of strongly enhanced visible light transmission through single C-shaped nanoapertures," Appl. Phys. Lett. **85**, 648-650 (2004).

#72378 - $15.00 USD Received 27 June 2006; revised 25 August 2006; accepted 28 September 2006

18. J. N. Farahani, D.W. Pohl, H.-J. Eisler, and B. Hecht, **"**Single Quantum Dot Coupled to a Scanning Optical Antenna: A Tunable Superemitter**,"** Phys. Rev. Lett. **95,** 017402 (2005).
19. L. Wang, S. M. Uppuluri, E. X. Jin, and X. Xu, "Nanolithography Using High Transmission Nanoscale Bowtie Apertures," Nano lett. **6**, 361-364 (2006).
20. E. X. Jin, and X. Xu, "Enhanced Optical Near Field from a Bowtie Aperture," Appl. Phys. Lett. **88**, 153110 (2006).
21. X. Xu, E. X. Jin, L. Wang, and S. M. Uppuluri, "Design, fabrication, and characterization of nanometer-scale ridged aperture optical antenna," Proc. SPIE **6106**, 61061J (2006).
22. A. Sundaramurthy, P. J. Schuck, N. R. Conley, D. P. Fromm, G. S. Kino, W. E. Moerner, "Toward Nanometer-Scale Optical Photolithography: Utilizing the Near-Field of Bowtie Optical Nanoantennas," Nano lett. **6**, 355-360 (2006).

1. Introduction

There is a continuous effort to develop nanolithography techniques for defining nanoscale features. Other than expensive electron beam lithography, a number of nanolithography techniques have been explored. These include near field photolithography [1,2], imprint nanolithography [3], scanning probe lithography [4] and surface plasmon assisted nanolithography [5-7]. A sub-wavelength hole in an opaque screen can be used to generate a small light source in the optical near field with nanometer scale optical resolution [8]. However, a nanometer-sized hole in circular or square shapes is plagued by low transmission and poor contrast [9]. The low transmission through regular nanoapertures can be ascribed to the waveguide cutoff effect. It is known that the fundamental cutoff wavelengths for the waveguides in circular and square cross sections are 1.7d and 2d (where d is either the diameter of the circular waveguide or the side length of the square waveguide), respectively. A sub-100 nm circular hole will be subjected to the cutoff conditions under UV or visible light illumination, therefore light can not be efficiently coupled through. This drawback limits regular nanoapertures from being employed in many applications.

Recently, numerical [10-15] and experimental [16-22] studies have demonstrated that ridge nanoapertures in C, H and bowtie shapes and bowtie antennas have the ability of achieving both enhanced light transmission and optical resolution better than the far field diffraction limit. As show in Fig. 1, the unique optical properties of ridge nanoapertures benefit from their specially designed geometries: two open arms and a nanometer-sized gap. When illuminated by light with proper polarization, the open arms endow the ridge aperture with long cutoff wavelengths which enable the propagation waveguide mode in the aperture, therefore boosting the transmitted light. The nanometer-sized gap confines the light through ridge aperture to a nanoscale spot in the near field, and therefore defines the achievable optical resolution. Hence, improved lithography performance of ridge nanoapertures over regular nanoapertures is expected [19] due to the aforementioned advantages.

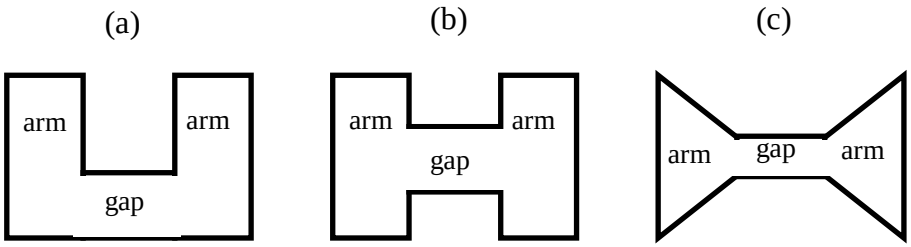

Fig. 1. (a) C, (b) H, and (c) bowtie shaped ridge apertures.

In this report, we focus on C-shaped ridge nanoapertures and show that the lithographic performance utilizing the enhanced transmission of C-shaped ridge nanoapertures can be used to produce sub -60 nm features in commercial photoresist using 355 nm excitation. Contact

#72378 - $15.00 USD Received 27 June 2006; revised 25 August 2006; accepted 28 September 2006

nanolithography experiments are conducted using C and regular apertures fabricated in the aluminum film as the contact mask. Only the C apertures are able to produce sub-60 nm features in photoresist, offering nanoscale optical resolution beyond the far field diffraction limit. It is therefore demonstrated that C aperture has much better performance over conventional rectangular and square apertures for nanolithography applications.

2. C aperture design and numerical simulation results

The gap size of the C aperture is determined by the desired optical resolution as well as fabrication capability. For example, based on FDTD calculations, a C aperture with a gap of 50 nm × 50 nm could provide a light spot as small as 60 nm × 60 nm at 20 nm below the aperture. It is also important to choose the right metal as the material of the opaque film, as it should have high reflection (to suppress the background light transmission through the metal film) and small skin depth (less loss for the light propagating through the aperture). Aluminum is selected as the film material because of its high reflectivity and small skin depth (reflectivity R = 0.92, skin depth δ = 6.5 nm) at the exposure wavelength of 355 nm. The aluminum film should be thick enough to completely block the background light in order to have a good contrast between the transmitted light propagating through the aperture and that penetrating through the film. The resonant condition of a C aperture can be obtained by computing and analyzing the spectral response of the designed aperture [10]. FDTD simulations considering the loss in aluminum using the Debye model (ε = -18.67 + 3.95i at 355 nm) as well as the dielectric constant of the photoresist layer underneath the mask (n = 1.6) are performed with illumination source polarized across the gap of the C aperture. A C aperture with 120 nm × 100 nm outline and 50 nm × 50 nm gap in a 120 nm thick aluminum film is found to have resonant transmission at the wavelength of 435 nm. A spectral response of the C aperture obtained by FDTD simulations is shown in Fig. 2. Transmission intensity is enhanced by a factor of eight at the resonance wavelength of 435 nm.

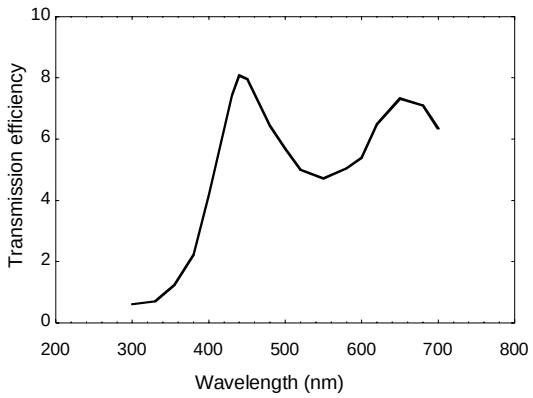

Fig. 2. Spectral response of C aperture with 120 nm × 100 nm outline and 50 nm × 50 nm gap in a 120 nm thick aluminum film. Transmission efficiency is defined by transmitted intensity integrated over the C aperture area normalized by the incident intensity integrated over the same area.

Because of the limitations on the photoresist and the laser wavelength, a 355 nm laser is used in this work for the lithography experiment. At this wavelength, the resonance will occur at much smaller bowtie geometry than we can currently fabricate. With the geometry used in this work, it is noted that even though 355 nm is not resonance wavelength, the transmission efficiency of the designed C aperture at 355 nm is still 1.24, much higher than a regular aperture of tens of nanometers (the small square aperture discussed below). It can be expected that there will be more significant enhancement in transmission efficiency if the resonant condition in C aperture can be achieved.

The C aperture with a 120 nm × 100 nm outline and a 50 nm × 50 nm gap, a 200 nm × 50

#72378 - $15.00 USD Received 27 June 2006; revised 25 August 2006; accepted 28 September 2006

nm rectangular aperture (REC) and a 100 nm × 100 nm square aperture (SQ) which have the same opening area as the C aperture, a 120 nm × 100 nm square aperture which has the same outline dimension, and a 50 nm × 50 nm small square aperture (SSQ) of the same gap size as the C aperture are simulated for the purpose of comparison. The incident light is polarized in the y-direction (the vertical direction in the figures). The material is a 120 nm-thick aluminum metal film and the thickness of the photoresist is 400 nm. Table 1 shows spot size, signal contrast, and transmission efficiency normalized to the incident intensity, which are critical parameters for lithography. It can be seen that C aperture shows significant advantages over other apertures in terms of achieving both field concentration and enhancement.

Table 1. Comparison of C and regular apertures

	C aperture	Rectangular aperture	Outline aperture	Square aperture	Small square aperture
Spot size at 20nmin the photoresist	60 nm × 60 nm	120 nm × 160 nm	100 nm × 180 nm	80 nm × 150 nm	50 nm × 100 nm
Signal Contrast	0.75	0.8	0.70	0.64	0.39
Transmission efficiency	1.24	1.86	1.21	0.43	0.002

Note: the spot size is defined by full width half magnitude (FWHM) of the electric field intensity, signal contrast is defined as $(I_{\max} - I_{\min})/(I_{\max} + I_{\min})$.

Figure 3 show the comparison among the fields transmitted through the apertures. Only the C aperture provides both field concentration and amplitude close to the incident field. For the REC aperture, since its cutoff wavelength is longer than 355 nm, a propagation mode is excited in the REC aperture; therefore, enabling a higher field output. However, the transmitted field is elongated in the y direction. For the SQ aperture in Fig. 2(c), it suffers from low transmission and the electrical field is mainly concentrated near the edges, which also makes the transmitted filed spread along the *y* direction. Figure 2(d) shows the SSQ aperture has very low transmission as expected.

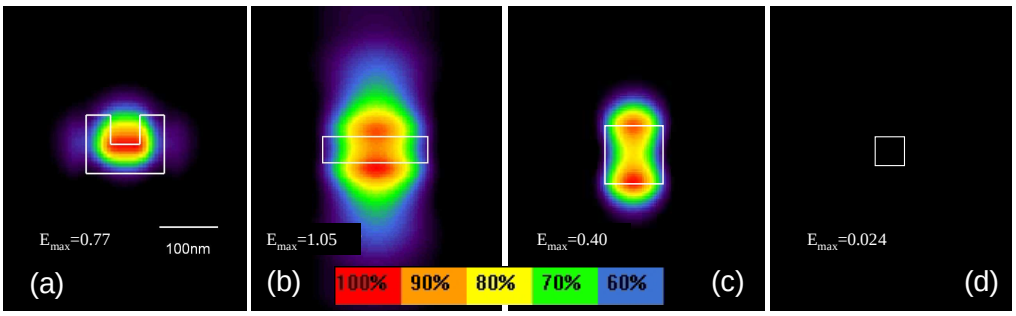

Fig. 3. Electrical field amplitude distribution normalized to the incident field at a distance 20 nm in the photoresist (a) C, (b) REC, (c) SQ, and (d) SSQ apertures

3. Experimental results and discussion

The lithography mask was fabricated on a 12.7 mm × 12.7 mm × 5 mm (thick) optically flat (30 nm overall flatness) quartz wafer. A thin 120 nm aluminum film was deposited on the quartz substrate by electron-beam evaporation. The roughness of the aluminum film,

#72378 - $15.00 USD Received 27 June 2006; revised 25 August 2006; accepted 28 September 2006

measured using an atomic force microscope (AFM), was found to be less than 8 nm over a 5 um × 5 um area. The mask was then fabricated by focused ion beam patterning. As shown in Fig. 4, a C aperture with the dimension used in the simulation, a 100 nm × 100 nm square aperture (SQ), a 200 nm × 50 nm rectangular aperture (REC), a 120 nm × 100 nm aperture (OU) which has the same outline dimension as the C aperture, and a 50 nm × 50 nm small square aperture (SSQ) were made in the same mask for the purpose of comparison.

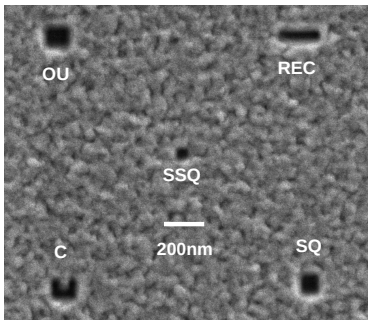

Fig. 4. SEM image of the lithography mask pattern.

Figure 5 shows the schematic diagram of the experimental setup for lithography. A diode pumped solid state (DPSS) laser at 355 nm wavelength is used as the exposure source. The polarization of the laser beam is directed across the gap of the C aperture so that the transmitted light can be concentrated underneath the gap. External force is applied onto the mask to provide the intimate contact between the mask and the resist sample. The experimental setup is housed in a class-10 glove box to minimize contamination and screen white light to prevent photoresist exposure. All apertures are illuminated simultaneously with a laser beam whose diameter is 110 μm, much larger than the overall dimension of the five apertures (1.5 μm x 1.5 μm); therefore, these apertures can be considered as illuminated under same conditions.

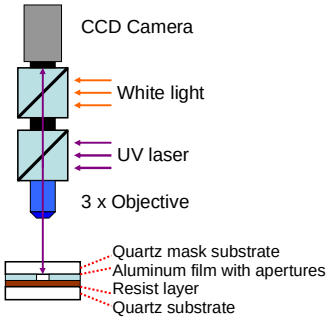

Fig. 5. Schematic diagram of the experimental lithography setup.

Shipley S1805 is used as the photoresist. Its thickness is 400 nm with the 5000 rpm spin-coating condition. As a light sensitive polymer, photoresist has a threshold exposure dose. Above this threshold dose, the exposed parts of the positive photoresist can be resolved by rinsing in the standard alkaline developer (Shipley MF321) for a short time (10 seconds), and holes (dimples) will be formed in the photoresist. Because the incident laser power density can be regarded as nearly uniform over the small area that contains all the apertures, the shape and size of the holes in the photoresist essentially characterize the transmission properties of the nano-apertures. In other words, with a given exposure time, the boundary of the holes formed by different apertures represents the iso-intensity profile of the transmitted light

#72378 - $15.00 USD Received 27 June 2006; revised 25 August 2006; accepted 28 September 2006

through individual apertures at the threshold dose. Obviously, longer exposure times will result in larger and deeper holes in the resist, thus it is important to control the exposure in order to obtain nanoscale holes. Precise control of the exposure was realized by varying the exposure time using an electric shutter in millisecond precision while fixing the laser output power. The laser intensity irradiating the mask is kept constant at 1.6 W/cm^2.

The results of the lithography experimental are summarized in Table 2. By varying the exposure time between 0.2 and 1.5 seconds, small holes from tens of nanometer to hundreds of nanometer in size are produced in the photoresist by C aperture, the outline aperture (OU), the square aperture (SQ) and the rectangular aperture (REC). The smallest square (SSQ) aperture did not produce any holes on the photoresist at any exposure time. The threshold dose is the minimum dose needed for the C aperture to produce lithography results, which should be at the edge of the hole formed by the C aperture. It is obtained as the product of the far field incident intensity, the exposure time, and the radio between the intensity at the edge of the hole formed by the C aperture and the incident intensity.

Table 2. Lithography results with varying exposure times.

Aperture	1.5 s	0.5 s	0.2 s
C (nm)	150 × 200	80 × 100	50 × 60
SQ (nm)	little irregular modification	Not developed	Not developed
OU (nm)	120 × 150	Partially developed shallow hole	Not developed
SSQ (nm)	Not developed	Not developed	Not developed
REC (nm)	220 × 300	150 × 250	130 × 220
Threshold dose	17.3 mJ/cm^2	18.2 mJ/cm^2	21.9 mJ/cm^2

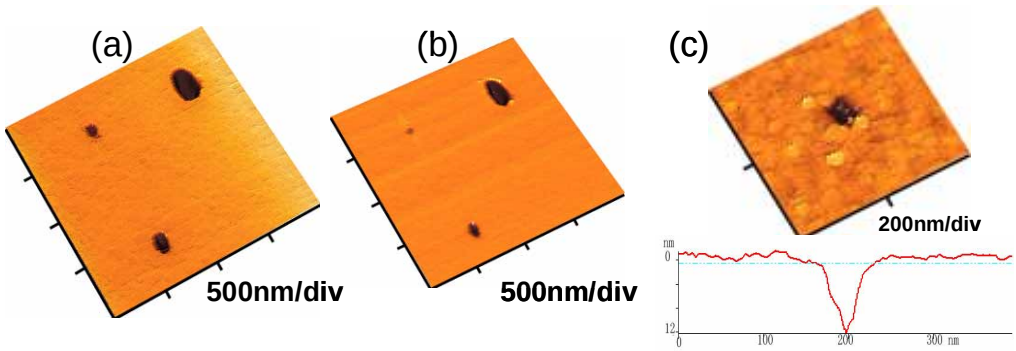

Fig. 6. AFM image of lithography results at 1.5 s (a) and 0.5 s (b) exposure time. (c) An enlarged image of lithography hole formed by the C aperture at a 0.2 s exposure time and its cross section profile.

For an exposure time of 1.5 s, holes with sizes of about 220 nm x 300 nm, 120 nm x 150 nm and 150 nm x 200 nm are formed by the REC aperture, the OU aperture and the C aperture, respectively. There is nothing from the SSQ aperture and little irregular modification of the photoresist surface is barely observed at the position of the SQ aperture, indicating the exposure doses obtained from these two apertures are less than the photoresist threshold

#72378 - $15.00 USD Received 27 June 2006; revised 25 August 2006; accepted 28 September 2006

value. The REC, OU and C apertures are all over-exposed because the lithography holes are larger than the outline dimensions of the apertures. Using a 0.5 s exposure time, the OU aperture produces partially developed shallow hole as shown in the AFM image in Fig. 6(b). Hole sizes from the C and REC apertures reduce to 80 nm x 100 nm and 150 nm x 250 nm, respectively. Nothing is produced by the SQ aperture. To further decrease the exposure dose, a 0.2 s exposure time is used. There is nothing formed by the OU aperture and the size of the hole produced by the REC aperture reduces to 130 nm × 220 nm. The hole formed by the C aperture is reduced to 50 nm × 60 nm in size, about 1/7 of the excitation wavelength. An enlarged AFM image of the hole produced by the C aperture with a 0.2 s exposure time is shown in Fig. 6(c). To examine the repeatability of the lithography, C apertures array were fabricated onto the same mask and were exposed in the same condition. Fig. 7 shows AFM image of the lithography holes produced by two C apertures obtained at 0.2 s exposure time and a cross sectional profile. Their size difference is less than 10%.

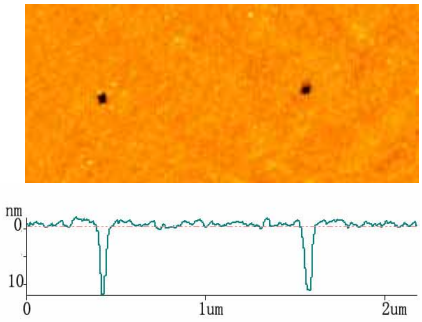

Fig. 7 AFM image and topography profile of C aperture array at 0.2 s exposure time

Experimental and FDTD results were compared by finding the threshold dose needed in the lithography experiments, and is explained below. As explained previously, the energy dose (in mJ/cm^2) at the edge of the hole produced in the resist represents the threshold value of photoresist exposure. To obtain the energy dose at the edge of the holes, FDTD calculations are conducted. The calculated intensity value (in mW/cm^2) at the experimentally determined edge of the hole is multiplied by the exposure time to obtain the threshold dose (in mJ/cm^2) as shown in Table 2. The mean value of the threshold doses is 19.6 mJ/cm^2. This value is of the same order of the threshold value measured independently using a (far field) lithography stepper, 7 mJ/cm^2. The discrepancy between the two may be due to the imperfect contact between the mask and the photoresist, which is not considered in the calculations. In addition, the calculation does not use the exact geometry of the apertures on the mask due to the uncertainty in the geometry measurements.

4. Conclusion

Optical transmission through C aperture and other apertures with regular shapes in a metal film are computed and compared using the FDTD method. The apertures are fabricated in a metal film and are used as a nanoscale light source for nanolithography. Holes with dimensions as small as 60 nm are produced in photoresist. The performance of the C apertures is compared with the apertures with regular shapes which demonstrates their advantages and potentials for nanolithography applications.

Acknowledgments

The financial supports to this work by the National Science Foundation and the Office of Naval Research are acknowledged. Fabrications of aperture samples by FIB were carried out in the Center for Microanalysis of Materials, the University of Illinois, which is partially supported by the U.S. Department of Energy.

#72378 - $15.00 USD Received 27 June 2006; revised 25 August 2006; accepted 28 September 2006